Vol. 571: 65–81, 2017
https://doi.org/10.3354/meps12135

MARINE ECOLOGY PROGRESS SERIES
Mar Ecol Prog Ser

Published May 17

Live benthic foraminifera in the Yellow Sea and the East China Sea: vertical distribution, nitrate storage, and potential denitrification

Zhaomeng Xu[1], Sumei Liu[1,2,*], Rong Xiang[3], Guodong Song[1,2,4]

[1]Key Laboratory of Marine Chemistry Theory and Technology MOE, Ocean University of China/ Qingdao Collaborative Innovation Center of Marine Science and Technology, Qingdao 266100, PR China

[2]Laboratory for Marine Ecology and Environmental Science, Qingdao National Laboratory for Marine Science and Technology, Qingdao 266100, PR China

[3]Key Laboratory of Marginal Sea Geology, South China Sea Institute of Oceanology, Chinese Academy of Sciences, Guangzhou 510301, PR China

[4]College of Chemistry and Chemical Engineering, Ocean University of China, Qingdao 266100, PR China

ABSTRACT: Benthic foraminifera were investigated to determine their vertical distribution, nitrate storage, and potential denitrification in the Yellow Sea (YS) and the East China Sea (ECS). The phytodetritus content and freshness as well as sediment redox conditions were key factors determining the vertical distribution of foraminifera in sediments of the YS and the ECS. The intracellular nitrate ($ICNO_3$) concentrations of *Nonionella stella*, *Hanzawaia nipponica*, *Bolivina robusta*, *Cancris auriculus*, and *Globobulimina pacifica* ranged from 3 to 114 mM, which in some cases was several hundred-fold more than the pore water nitrate ($PWNO_3$) concentrations. The genus *Hanzawaia* was for the first time reported to store $ICNO_3$ (316 ± 73 pmol ind.$^{-1}$; 11 ± 3 mM). The significant correlation between the $ICNO_3$ concentration and foraminiferal abundance (Pearson correlation: r = 0.401, p < 0.01, n = 60) suggested that foraminifera may have an important role in nitrate storage in the sediments. The foraminiferal intracellular nitrate ($FINO_3$) pool ranged from 9 to 74% of the $ICNO_3$ pool in sediments, indicating that nitrate may be stored by other sediment organisms (e.g. diatoms). The chlorophyll *a* concentration, chloroplastic pigment equivalents (CPE), and chlorophyll *a*:phaeopigment ratio were all significantly positively correlated with the $ICNO_3$ concentration (Pearson correlation: r = 0.563, 0.603, and 0.457, respectively; p < 0.01; n = 60), indicating that phytodetritus (e.g. diatoms) might also contribute to sedimentary $ICNO_3$. Potential foraminiferal denitrification rates ranged from 9 to 92 µmol m^{-2} d^{-1} in the YS and the ECS, indicating that benthic foraminifera might play a role in sedimentary denitrification.

KEY WORDS: Live benthic foraminifera · Vertical distribution · Intracellular nitrate · Potential denitrification · Yellow Sea · East China Sea

INTRODUCTION

Nitrate is a key limiting nutrient for primary production and also has a significant role in marine biogeochemical cycles (Gruber 2004, Arrigo 2005). However, anthropogenic activities have resulted in the release of large quantities of nutrients (including nitrate) to the ocean from rivers, groundwater, wastewater discharges, and atmospheric deposition, and eutrophication has become a major problem in coastal ecosystems (Turner & Rabalais 1994, Humborg et al. 1997, Turner et al. 2003, Zhang et al. 2007a). Denitrification in sediments is a crucial process that can alleviate the effects of excessive nitrate in eutrophic aquatic ecosystems (Seitzinger 1988).

*Corresponding author: sumeiliu@ouc.edu.cn

The recent discovery that benthic foraminifera can use nitrate as an electron acceptor for denitrification has broadened understanding of anaerobic metabolism in eukaryotes and their role in the nitrogen cycle (Risgaard-Petersen et al. 2006, Piña-Ochoa et al. 2010a). The contribution of potential foraminiferal denitrification to the total removal of nitrate ranges from 4% (Sagami Bay, Japan; Glud et al. 2009) to >70% (Bay of Biscay and Chile oxygen minimum zones; Piña-Ochoa et al. 2010a). In some environments, foraminifera contribute substantially to benthic denitrification, and their contribution can exceed that of prokaryotes (Kamp et al. 2015). These discoveries have challenged some previous studies and have renewed interest in understanding and quantifying the turnover of benthic nitrogen. The intracellular concentration of nitrate in benthic foraminifera can be several hundred-fold greater than that of their environment, enabling them to be independent of an electron acceptor (nitrate) supply in anoxic marine environments (Bernhard 1992, Gooday et al. 2000, Risgaard-Petersen et al. 2006, Høgslund et al. 2008, Glud et al. 2009, Piña-Ochoa et al. 2010a, Prokopenko et al. 2011, Koho & Piña-Ochoa 2012, Glock et al. 2013). Due to the capacity of nitrate storage, foraminifera can also take part in nitrate bio-transport, which has been shown to transport nitrate to increase fixed nitrogen losses and to decrease the efficiency of organic carbon burial in suboxic and anoxic sediments (Prokopenko et al. 2011, Dale et al. 2016).

Continental margin sediments are considered to be a large sink for fixed nitrogen in the oceans (Middelburg et al. 1996). The Yellow Sea (YS) and East China Sea (ECS) are marginal seas (average depth: 72 m) bounded by mainland China, the Korean Peninsula, the Ryukyu Islands, and Taiwan, in the northwest Pacific Ocean. Both seas are characterized by the input of large amounts of anthropogenic nutrients, and high levels of primary productivity (Gong et al. 2003, Liu et al. 2009). Nitrate storage has also been implied in sediments of the ECS (Song et al. 2013). However, few studies have attempted to address the vertical distribution of benthic foraminifera, their storage of nitrate, and the potential contribution they make to denitrification in sediments of the YS and the ECS. We investigated the total standing stock, assemblages, vertical distribution, and intracellular nitrate ($ICNO_3$) of common benthic foraminiferal species. To investigate their role in the sediment nitrogen cycle of the YS and the ECS, we also quantified the inventory of the pore water nitrate ($PWNO_3$) pool, $ICNO_3$ pool, and foraminiferal intracellular nitrate ($FINO_3$) pool and calculated the potential foraminiferal denitrification rates.

MATERIALS AND METHODS

Sites and sampling

Sediments were collected during July 2013 at Stns C05, A02, F11, and ME3 using a multi-corer (4 Plexiglas tubes with inner diameter of 9 cm, length of 60 cm) and at Stns B5 and M7 during August 2013 using a box corer in the YS and the ECS (Fig. 1). For the multi-corer, the sediment cores were directly collected when it was recovered, while for the box corer, sediment sub-cores were obtained by manually inserting Plexiglas tubes to withdraw the sub-cores. Only sediment cores/sub-cores having an undisturbed surface were selected for subsequent procedures, including the collection of live benthic foraminifera, pore water extraction, foraminiferal faunal analysis, and measurement of sediment physicochemical properties, including porosity, sediment phytopigments, total organic carbon (TOC), and total nitrogen (TN). All cores were sliced horizontally at 1 cm intervals (0–10 cm) immediately following collection, with the exception of the cores for pore water extraction from Stns M7 and C05, which

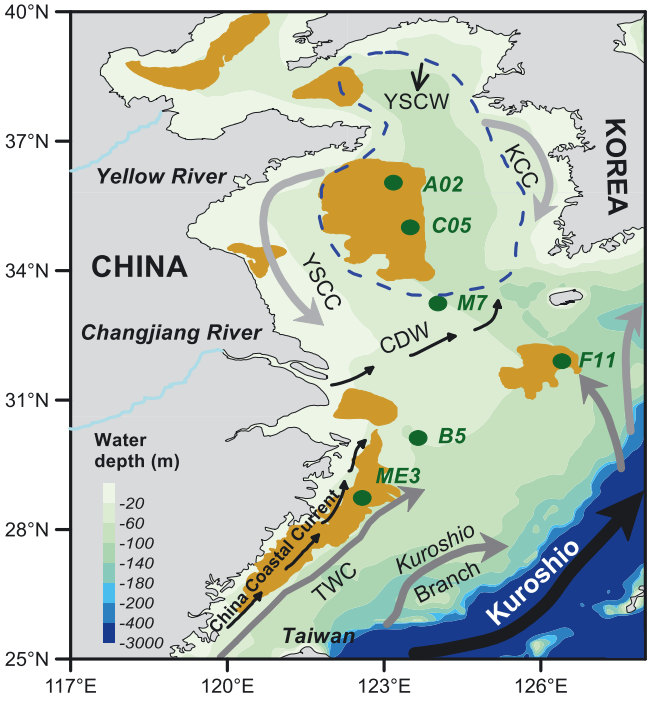

Fig. 1. The study area and geographical locations of the 6 sampling stations during summer 2013. The area inside the blue dashed line represents the Yellow Sea Cold Water (YSCW). Orange patches represent mud areas (Hu et al. 2012). The main water masses are also delineated (Guan 1994). YSCC: Yellow Sea Coastal Current; KCC: Korean Coastal Current; TWC: Taiwan Warm Current; CDW: Changjiang Diluted Water

were sliced at 0.5 cm intervals (0–5 cm) and 1 cm intervals (5–10 cm). Near-bottom water samples for sieving of the live foraminifera and determination of basic environmental parameters were collected in 10 l Niskin bottles attached to a Seabird CTD-rosette system.

Chemical and physical analysis

Environmental parameters

The temperature, salinity, water depth, and dissolved oxygen (DO) content of near-bottom water were measured using a CTD sensor (Table 1). DO concentrations were also measured by Winkler titration to calibrate the oxygen sensor of CTD. Pore water was immediately extracted (Unfrozen extraction) from the sliced sediments, using Rhizon samplers (Seeberg-Elverfeldt et al. 2005, Liu et al. 2011). Samples of water overlying the sediment surface were collected and filtered using 0.45 µm syringe filters. The overlying and pore water samples were preserved at −20°C until analysis. The nitrate concentrations of overlying and pore water were measured using the VCl_3 reduction method (Braman & Hendrix 1989) and chemiluminescence detection (Model 200E; Teledyne Advanced Pollution Instrumentation). Furthermore, for the purpose of measuring the oxygen penetration depth (OPD) in the sediment, 3 small sub-cores were removed using a cut-off syringe (inner diameter: 3 cm) from single cores collected at Stns A02, C05, and M7 in another field study undertaken during August 2015. Sediment pore water DO profiles were measured within 1 h of collection using an oxygen microelectrode (OX-25; Unisense, Denmark) having a resolution of 100 µm. Due to ex-situ measurement, the cores may have potentially been contaminated by oxygen in the air before determination, so the measured OPD may be higher than the actual values.

Sediments sliced for measurement of physico-chemical properties were preserved at −20°C in the dark and freeze dried before analysis. The sediment water content was determined by weight difference (measurements made before and after freeze-drying), and the sediment porosity (φ) was calculated from the water content, assuming a bulk sediment density of 2.5 g cm^{-3} (Song et al. 2013). The sediment TOC and TN were measured using an elemental analyzer following the procedure of Zhang et al. (2007b). Prior to analysis, the sediment was ground using an agate mortar and pestle and acidified with HCl to remove inorganic carbon. The sediment phyto-pigments chlorophyll *a* (chl *a*) and phaeopigments (Phaeo) were extracted into a 90% acetone solution (Yentsch & Menzel 1963) and measured using a Hitachi F4500 fluorimeter, following the method of Shuman & Lorenzen (1975). Chloroplastic pigment equivalents (CPE), representing chl *a* + Phaeo, were used as an indicator of food availability (Thiel 1978). The chl *a*: Phaeo ratio was used to estimate the freshness of organic matter for foraminifera use as a food resource.

$ICNO_3$ storage in foraminifera

Freshly sliced sediment for picking up live foraminifera to measure $ICNO_3$ was sieved immediately on board the vessel through a 150 µm mesh screen, using filtrated near-bottom water, and the material retained in the sieve was transferred to a Petri dish. Live foraminifera were collected from the material using a stereomicroscope, based on the presence of different cytoplasmic colors and organic matter gathered around the aperture. The length (*L*), width (*W*), and thickness (*T*) of each foraminifer were measured using the stereomicroscope. Foraminiferal individuals selected for nitrate analysis were cleaned using a brush, washed 3 times by sequential transfer to low-oxygen and nitrate-free aged seawater in Petri dishes, then transferred to PCR tubes that were sealed and

Table 1. Biogeochemical properties of near-bottom seawater and sediments at 6 stations. TOC: total organic carbon; DO: dissolved oxygen. OPD: oxygen penetration depth

Station	Latitude (N)	Longitude (E)	Depth (m)	Near-bottom water temp. (°C)	Near-bottom water salinity	Near-bottom water DO (µM)	Surface sediment TOC (%)	OPD (cm)
A02	123° 10.708′	36° 02.293′	73	8.30	32.20	213	1.37	0.37 ± 0.02
C05	123° 30.071′	35° 00.134′	78	9.14	32.88	220	1.09	0.69 ± 0.04
M7	124° 01.814′	33° 14.335′	66	10.35	32.93	197	0.65	0.26 ± 0.03
F11	126° 24.207′	31° 54.027′	97	20.34	33.91	181	0.79	–
B5	123° 39.080′	30° 07.283′	67	21.52	34.17	152	0.35	–
ME3	122° 34.904′	28° 43.931′	63	18.37	34.41	159	0.85	–

stored at −20°C until analysis. The $ICNO_3$ of foraminiferal individuals was extracted in the PCR tubes by the addition of 20 µl of NaOH solution (10%) (Piña-Ochoa et al. 2010a). The nitrate content in the extract was also measured using the chemiluminescence method, for which the relative deviations of parallel determinations were <3% (n = 5) and the analytical limit of detection was <10 pmol. Dead empty foraminiferal tests were treated using the same procedure, as contamination controls. To calculate foraminiferal volumes, each species was regarded as an ideal geometric shape, based on its morphology. For example, *Globobulimina pacifica* was treated as an oblate elliptical cone ($1/8\pi L[1/2W]^2$), *Nonionella stella* was treated as an oblate spheroid ($4/3\pi[1/2L]^2[1/2W]$), *Hanzawaia nipponica* and *Cancris auriculus* were treated as elliptic cylinders ($1/4\pi LWT$), and *Bolivina robusta* was treated as a prolate spheroid ($4/3\pi[1/2L][1/2W]^2$). The resulting volumes and nitrate contents were used to calculate the $ICNO_3$ concentrations for each foraminiferal individual.

Methods for releasing the $ICNO_3$ pool

Four extraction methods were used to determine the $ICNO_3$ pool at Stn ME3. Each section of sediment (1 cm sections over the range 0–10 cm) was mixed to ensure homogeneity, and 1 ml samples were transferred to each of 5 centrifuge tubes. In the first method (KCl extraction), 5 ml 1 M KCl was added to the tube, the mixture was shaken vigorously for 2 min and extracted using a Rhizon sampler, and subsequently the extract was transferred to a centrifuge tube and stored at −20°C. In the second method (DW extraction), the procedure was the same as in the KCl extraction method, but deionized water (DW) was used instead of 1 M KCl. The KCl and DW extraction methods were adepted from Sayama (2001) and aimed to change the cellular osmotic pressure to release $ICNO_3$. Because $ICNO_3$ can be released during pore water extraction using centrifuging (Larsen et al. 2013), we used Rhizon samplers in all of the extraction methods, rather than centrifugation. In the third method (NaOH extraction), the procedure was the same as in the KCl extraction method, but 1 M NaOH was used instead of 1 M KCl. In the fourth method (Frozen extraction), the sediment in the centrifuge tube was frozen at −20°C for <1 mo, then thawed in boiling water for 10 min and extracted using a Rhizon sampler (Risgaard-Petersen et al. 2006). The NaOH and Frozen extractions aimed to destroy the cell membrane and so release $ICNO_3$. At the other stations, we used the Frozen extraction method to release the $ICNO_3$ pool. The nitrate concentrations were measured using the chemiluminescence method described above.

Foraminiferal faunal analysis

Benthic foraminifera typically inhabit the top 10 cm of sediments, with different species occurring at specific sediment depths and in particular microhabitats (Corliss 1985, Gooday 1986). In this study, the foraminiferal assemblages and vertical distribution were determined in the top 0–10 cm of the sediment. The sliced sediments for foraminiferal faunal analysis were transferred into PVC bottles, stained, and preserved in a solution of Rose Bengal in 95% ethanol solution (1 g l^{-1}) (Walton 1952) until further treatment. In the laboratory, each sample was sieved through a 150 µm mesh, and the material retained on the sieve was stored in 95% ethanol with Rose Bengal (1 g l^{-1}). Stained foraminifera in the 150 µm size fraction were placed in solution (50% ethanol and 50% water) for sorting. The Rose Bengal staining technique (Walton 1952, Bernhard 1988) is commonly used to distinguish live and dead foraminifera. A potential problem in this method is that Rose Bengal can stain the protoplasm of dead undecomposed foraminifera in anoxic sediment (Corliss & Emerson 1990, Bernhard 2000). We therefore applied strict staining criteria and compared doubtful individuals with perfectly stained individuals of the same species collected in surface sediment layers. Non-transparent agglutinated and miliolid taxa were crushed to distinguish the test interior. Arborescent and tubular fragile foraminiferal fragments were not included.

Faunal diversity values were expressed using the Shannon (H; Eq. 1) and Evenness (E; Eq. 2) indices (Shannon 1948, Hayek & Buzas 1997), as described by Murray (2006). To describe the vertical distribution of the foraminiferal community or individual taxa, we use the average living depth (ALD; Eq. 3) (Jorissen et al. 1995).

$$H = -\sum_{i=1}^{i=S} (n_i/N) \times \ln(n_i/N) \quad (1)$$

$$E = e^H/S \quad (2)$$

$$ALD_{10} = \sum_{i=1}^{i=10} (N_j D_j)/N \quad (3)$$

In the above equations, n_i is the number of individuals of species i in the entire core (0–10 cm), N is the total number of foraminiferal individuals for all sediment intervals (0–10 cm), S is the number of

species, N_j is the total number of individuals in each sediment interval, and D_j is the midpoint depth of the sample interval *j*.

Calculation

Inventories of $PWNO_3$ pool and $ICNO_3$ pool

The inventories of the $PWNO_3$ and $ICNO_3$ pools were calculated according to Eqs. (4) & (5):

$$PWNO_3 = \sum_{i=0,10} C_i^{Unfrozen} \times V_i \times \varphi_i \quad (4)$$

$$ICNO_3 = \sum_{i=0,10} (C_i^{Frozen} - C_i^{Unfrozen}) \times V_i \times \varphi_i \quad (5)$$

where $C_i^{Unfrozen}$ is the $PWNO_3$ concentration in each sediment layer associated with the Unfrozen extraction, C_i^{Frozen} is the $PWNO_3$ concentration in each sediment layer associated with the Frozen extraction (designed to release the $ICNO_3$ pool), V_i is the volume of each sediment layer, and φ_i is the porosity of each sediment layer (Fig. S1 in the Supplement at www.int-res.com/articles/suppl/m571p065_supp.pdf). In the calculations, the superficial area of the sediment core was normalized to 1 m^2.

Inventory of $FINO_3$ pool

The inventory of the $FINO_3$ pool was estimated based on the abundance of particular foraminiferal species in the sediments from 0 to 10 cm depth, normalized to 1 m^2; this value was multiplied by the cytoplasm nitrate content for that species. The nitrate content in cells of the foraminifera *N. stella, H. nipponica, B. robusta, C. auriculus,* and *G. pacifica* are shown in Table 2. We did not measure the nitrate content of the foraminiferal species *Fursenkoina schreibersiana*, *Bulimina marginata*, and *Stainforthia complanata* but used the values for the genera involved, reported by Piña-Ochoa et al. (2010a) and Bernhard et al. (2012). The specific nitrate content of the various foraminiferal species is shown in Table 2. Eq. (6) shows the formula for calculating the community $ICNO_3$:

$$FINO_3 = \sum_{i=a,b,c\ldots} A_i \times C_i \quad (6)$$

where *a*, *b*, and *c* (etc.) represent the $ICNO_3$ stores for various foraminiferal species, C_i is the nitrate content for a particular foraminiferal species, and A_i is the abundance of a particular foraminiferal species in the integrated core sediments (normalized to 1 m^2).

Potential foraminiferal denitrification rates

The individual denitrification rates for approximately 11 foraminiferal species have been measured, but for most species, these data are unknown (Risgaard-Petersen et al. 2006, Piña-Ochoa et al. 2010a, Bernhard et al. 2012). We used the estimation method of Glock et al. (2013), and 2 assumptions (A and B) to determine potential foraminiferal denitrification rates in our study. Assumption A was that, where the species-specific denitrification rate is unknown, the average denitrification rate reported for a particular genus is applicable generally to species in that genus, provided that they occupy a similar ecological niche. Assumption B was that species from genera with unknown denitrification rates would have a similar denitrification capacity. The proportions of species from genera with unknown denitrification rates were added into the potential total foraminiferal denitrification rate (TFDR). For the various foramini-

Table 2. Intracellular nitrate content and concentration in individual foraminifera. SBB: Santa Barbara Basin; OMZ: oxygen minimum zone

Foraminiferal species	No. of ind.	Intracellular nitrate content (pmol ind.$^{-1}$) ± SEM	Volume (10^{-3} mm^3)[a]	Intracellular nitrate concentration (mM)[a]	Site	Reference
Nonionella stella	7	162 ± 27	53 (3.9)	3 (0.6)	C05, Yellow Sea	This study
Hanzawaia nipponica	5	316 ± 73	30 (0.52)	11 (3)	C05, Yellow Sea	This study
Bolivina robusta	5	212 ± 46	6.1(0.38)	35 (6)	M7, Yellow Sea	This study
Cancris auriculus	4	3211 ± 1046	28 (5.1)	114 (23)	B5, East China Sea	This study
Globobulimina pacifica	3	1167 ± 455	75 (7.0)	16 (5)	F11, East China Sea	This study
Arenoparella asiatica	5	0	9.5 (0.86)	0	C05, Yellow Sea	This study
Fursenkoina cornuta	2	796 ± 809	–	–	SBB, California, USA	Bernhard et al. (2012)
Bulimina marginata	14	40 ± 4	32 (1.1)	4 (1)	Bay of Biscay	Piña-Ochoa et al. (2010a)
Stainforthia sp.	26	60 ± 46	0.33 (0.021)	180 (29)	OMZ, Chile	Piña-Ochoa et al. (2010a)

[a]SEM is given in parentheses

feral species in our study, the specific denitrification rates used to calculate the denitrification rates for those species are shown in Table 3. In this study, the OPD was all <1 cm at Stns A02, C05, and M7. Foraminifera may rely on aerobic respiration in the surface oxic sediments rather than denitrification (Piña-Ochoa et al. 2010a). Therefore, we calculated the maximum potential total foraminiferal denitrification rates ($TFDR_{max}$) by including foraminifera in the 0–1 cm sediment layer as the upper limit, and the minimum potential total foraminiferal denitrification rates ($TFDR_{min}$) excluding foraminifera in the 0–1 cm sediment layer as the lower limit. This method produces a range of the potential TFDR at each station. By applying the species-specific denitrification rates (Table 3) to the abundances of particular foraminiferal species in sediment core including or excluding the 0–1 cm sediment layer, $TFDR_{max}$ or $TFDR_{min}$ for each site was estimated as:

$$TFDR = (1 + A_{unknown}/A_{known}) \sum_{i=a,b,c\ldots} A_i \times R_i \quad (7)$$

where *a*, *b*, and *c* (etc.) are the various foraminiferal species with known denitrification rates. R_i is the individual denitrification rate for particular foraminiferal species (Table 3), and A_i is the specific foraminiferal species abundance in the sediment core including or excluding the 0–1 cm sediment layer, normalized to 1 m^2. $A_{unknown}$ or A_{known} is the total abundance of foraminiferal species with unknown or known individual denitrification rate, respectively, in the core sediments (including or excluding the 0–1 cm sediment layer), normalized to 1 m^2.

RESULTS

Sediment environmental parameters

Sediment redox conditions

The near-bottom water DO concentration ranged from 152 µM at Stn ME3 to 220 µM at Stn C05 (Table 1). All stations were characterized by oxic near-bottom water conditions. The near-bottom water temperature was significantly negatively correlated with the near-bottom water DO (Pearson correlation: $r = -0.908$, $p < 0.05$, $n = 6$). The OPD was <1 cm at stations where measurements were made (Table 1, Fig. S2 in the Supplement), which indicates that anoxic conditions formed in the 0 to 1 cm sediment layer. The nitrate concentrations peaked at the sediment surface at Stns A02 and M7, and in the sediment sub-surface at Stns C05, F11, and B5 (Fig. 2). Stn ME3 had the deepest nitrate penetration depth (NPD; 5.5 cm), and the nitrate concentration was approximately 4 µM in the 0 to 4 cm depth layer (Fig. 2). At the other stations, the NPD was at approximately 2 to 3 cm, except for Stn F11.

Table 3. Referenced denitrification rates for specific foraminiferal species

Foraminiferal species	Denitrification rates (pmol nitrogen $ind.^{-1}$ d^{-1})
Nonionella stella[a]	84
Globobulimina pacifica[a]	565
Stainforthia sp.[b]	70
Bolivina robusta[b]	124
Fursenkoina schreibersiana[c]	1386

[a]Risgaard-Petersen et al. (2006); [b]Piña-Ochoa et al. (2010a); [c]Bernhard et al. (2012)

Sediment biochemical composition

The TOC content of surface sediments ranged from 0.35% to 1.37% (Table 1). Higher values (>1%) were recorded at Stns A02 and C05, which were located in mud areas of the YS (Fig. 1). The minimum TOC content (Table 1) and porosity (Fig. S1) both occurred at Stn B5. The TOC and TN contents showed a general decrease with sediment depth at all stations except Stn F11 (Fig. 3). Although the TOC content was higher in surface sediments at Stn F11 compared with Stns B5 and M7, the chl *a* concentrations, CPE, and chl *a*:Phaeo ratio in surface sediments were lowest at Stn F11 (Fig. 4). The maximum chl *a*:Phaeo ratio for surface sediments was found at Stn M7. The chl *a* concentrations, CPE, and chl *a*:Phaeo ratio generally decreased with sediment depth at all stations except Stn F11 (Fig. 4).

Foraminiferal assemblages and vertical distribution

At Stn A02, a total of 1940 live stained individual foraminifera were collected from the core; amongst these, the diversity index was $H = 1.09$, and evenness was $E = 0.37$ (Table 4). The maximum density (600 ind. 50 cm^{-3}) occurred in the top 1 cm (Fig. 5). The ALD_{10} for the total assemblage was 2.5 cm. The assemblage was dominated by *Protelphidium tuberculatum* (59%), with other abundant species being *Hanzawai nipponica* and *Nonionella stella*.

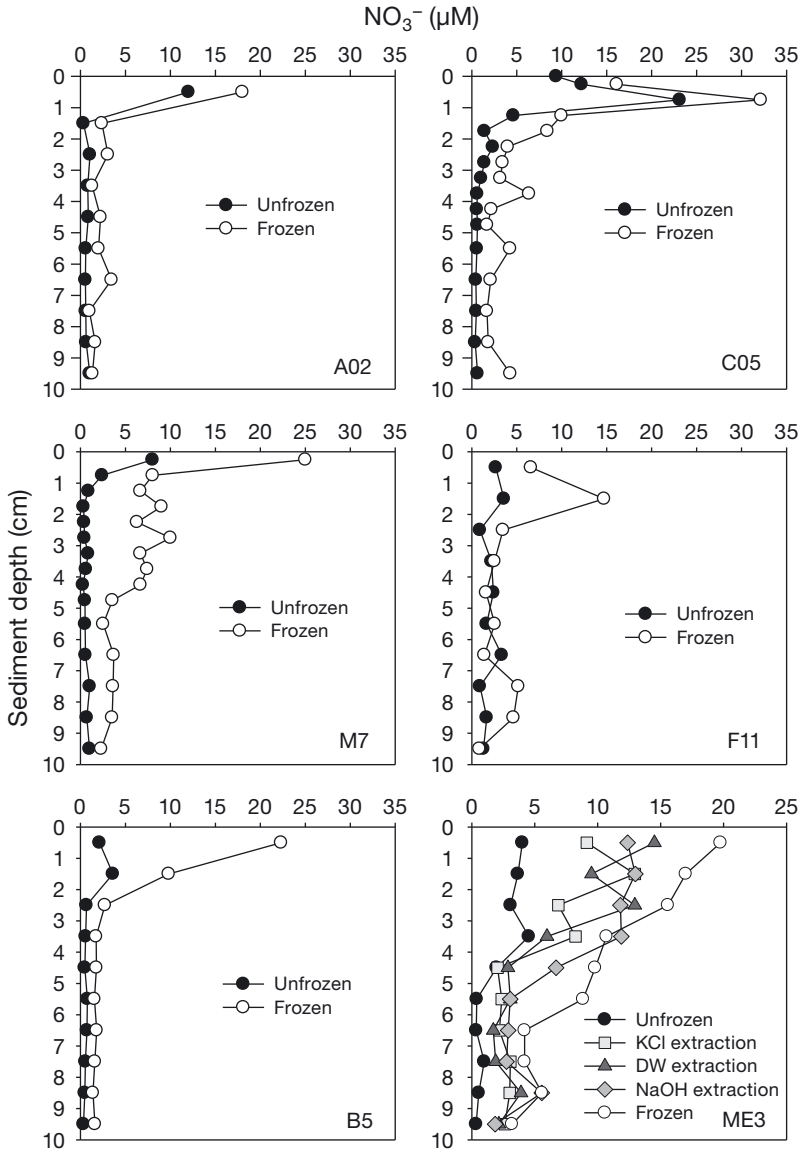

Fig. 2. Vertical distribution of pore water nitrate concentrations, based on various extraction methods. Unfrozen: the pore water was immediately extracted using on-board Rhizon samplers. Frozen: sediment was frozen at −20°C, and within 1 mo of freezing, the sediment was immersed in boiling water for 10 min, then extracted using a Rhizon sampler. DW: deionized water. The difference in nitrate concentrations between samples processed using the Unfrozen and Frozen methods was used to calculate the total intracellular nitrate pool in the sediments. The relative deviations of parallel determinations were <3% (n = 5)

For Stn C05 (total of 1180 stained foraminiferal individuals collected), there was a bimodal vertical distribution (Table 4, Fig. 5), with 1 peak in foraminiferal density found in the top 1 cm of sediment, and a second (70 ind. 50 cm^{-3}) at approximately 6–7 cm depth. *N. stella*, *Arenoparrella asiatica*, and *H. nipponica* were the major components, with maximum abundances at approximately 1.5, 0.5, and 6.5 cm depth, respectively.

Stn M7 had the highest density of foraminifera (3022 stained individuals; Table 4). The density was highest in the top 1 cm, but decreased rapidly with increasing sediment depth (Fig. 5); a total of 25 species were found, and the Shannon diversity index was relatively low. The extremely low evenness (E = 0.18) indicates that the assemblage was dominated by the species *Bolivina robusta* (53%) but included other species (*A. asiatica*, *Astrononion tasmanensis*, and *Cancris auriculus*). The ALD_{10} was 0.6 cm, and most species were present in the 0–1 cm interval. However, *B. robusta*, *C. auriculus*, and *Bulimina marginata* also occurred in microhabitats as deep as 10 cm.

Stn F11 is situated in the mud area southwest of Cheju and had the lowest abundance of foraminifera (355 stained individuals.) The abundance was highest at approximately 5–6 cm depth. The assemblage was characterized by the dominance of *B. robusta* (25%), *H. nipponica* (23%), *C. auriculus* (13%), and *B. marginata* (10%), and all these species occupied deep-infaunal habitats. The ALD_{10} for the total assemblage was 4.5 cm. The diversity index and evenness were comparable to Stn C05.

The core from Stn B5 yielded 1026 foraminifera. The maximum abundance was in the top 1 cm, the ALD_{10} of the total assemblage was 2.4 cm, and the Shannon diversity index was maximum. The assemblage was characterized by the dominance of *C. auriculus* (26%).

Stn ME3 is located in the Zhejiang coast mud zone and yielded 2868 individuals with vertical abundance showing a bimodal distribution. One density maximum was in the top 1 cm of sediments, and the second maximum (300 ind. 50 cm^{-3}) was at approximately 7–8 cm depth. The ALD_{10} (5.1 cm) for this station was the deepest among all stations. The diversity index and the evenness values were comparable to those for Stn M7. *Ammonia beccarii* (40%), *B. robusta* (31%), *Florilus cf. atlanticus* (12%), and *B. marginata* (5%) (Table S1, Fig. 5) were the dominant species,

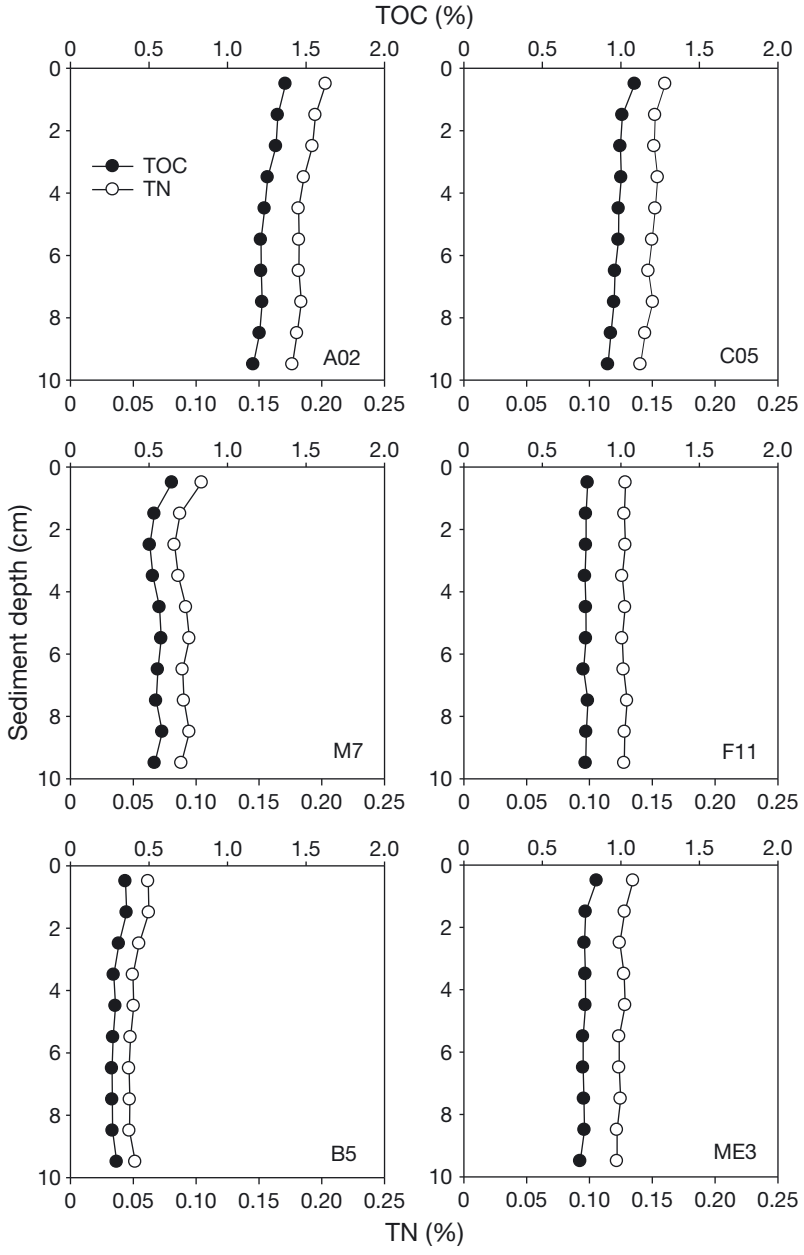

Fig. 3. Vertical distribution of the total organic carbon (TOC) and total nitrogen (TN) in sediments

and the occurrences of *A. beccarii* and *B. robusta* were mainly responsible for the bimodal vertical distribution, as they were present in both the top 1 cm and in the 6–8 cm layer.

The $FINO_3$ pool

Five foraminiferal species contained high $ICNO_3$ concentrations (Table 2). The nitrate concentration in these species was >100-fold the maximum concentration in adjacent pore water (Table 2, Fig. 2). *C. auriculus* collected at Stn B5 had the highest concentration of $ICNO_3$ (3211 ± 1046 pmol ind^{-1}) (Table 2). *Globobulimina pacifica*, which had the largest volume amongst the foraminifera, had the second highest concentration (1167 ± 455 pmol $ind.^{-1}$). *H. nipponica* also had a high concentration of $ICNO_3$ (316 ± 73 pmol $ind.^{-1}$; 11 ± 3 mM) and was present at most stations; this is the first report of the accumulation of $ICNO_3$ in this genus. We also compared the inventories of $FINO_3$ pool and $PWNO_3$ pool (Table 5) and found that the latter was higher at most stations. However, the $FINO_3$ pool was almost 2-fold greater than the $PWNO_3$ pool at Stns M7 and B5 (Table 5).

The $ICNO_3$ pool

At Stn ME3, the DW, KCl, and NaOH extraction methods all resulted in the release of $ICNO_3$ into the sediment, causing a marked increase in the pore water nitrate concentration (Fig. 2). The nitrate concentration in pore water following use of these extraction methods was approximately 2- to 3-fold that based on the Unfrozen extraction method at 0–4 cm depth, and approximately 4 µM below the NPD. Compared with 4 extraction methods at Stn ME3, the Frozen extraction method released the most $ICNO_3$ in almost every sediment layer (except 3–4 cm), and it also resulted in obvious $ICNO_3$ release at the other stations.

Comparison of the difference in nitrate concentrations determined based on the Frozen and Unfrozen extraction methods (Fig. 2) enabled calculation of the vertical distribution of $ICNO_3$ stores. There was a large concentration of $ICNO_3$ in almost all sediment layers from Stn ME3, and the concentrations decreased with sediment depth. $ICNO_3$ storage occurred in the uppermost sediment layer at all stations and was also evident in the sub-surface sediments at Stns C05 and M7, even below the NPD. The inventory of $ICNO_3$ pool far exceeded that of the $PWNO_3$ pool at some

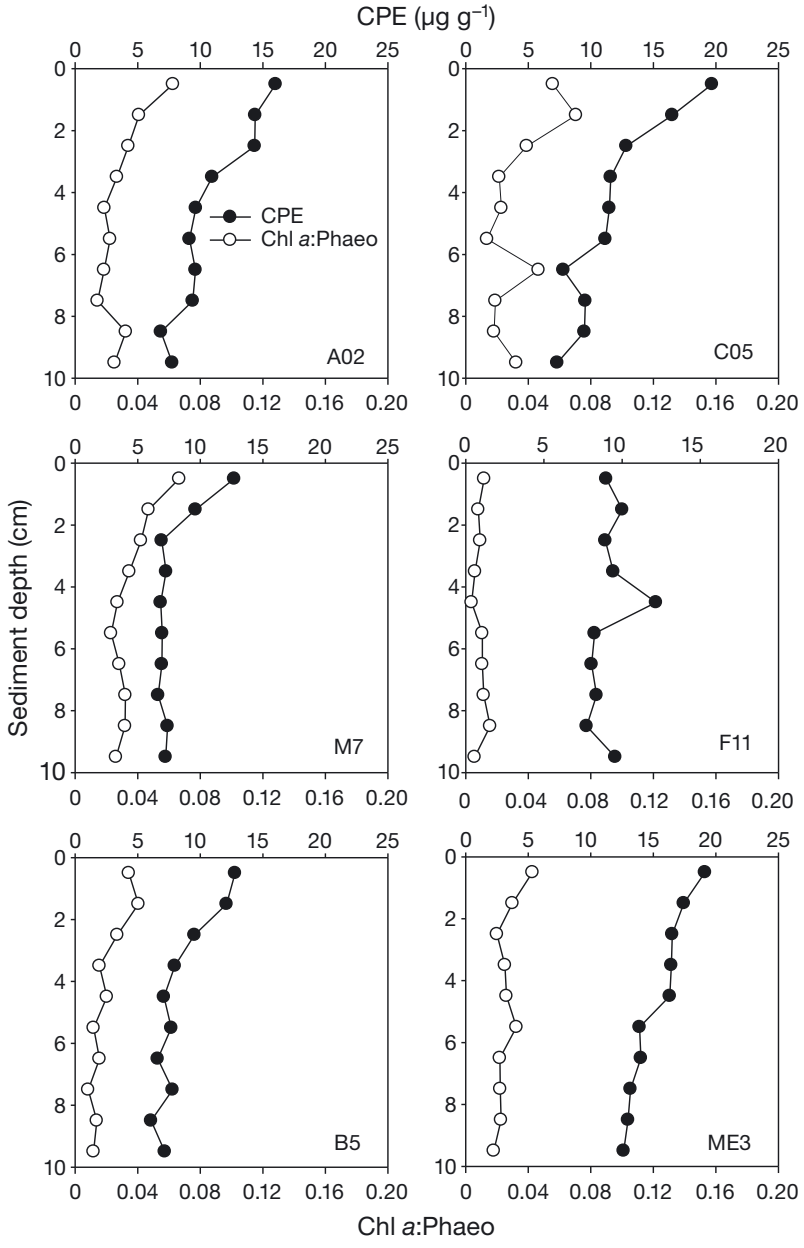

Fig. 4. Vertical distribution of the chloroplastic pigment equivalents (CPE; Thiel 1978) and chlorophyll *a*:phaeopigment (chl *a*:Phaeo) ratio in sediments from the 6 stations. The chl *a*:Phaeo ratio was used to estimate the freshness of the food available to the foraminifera

Table 4. Foraminiferal biotic variables at 6 stations. ALD_{10}: the foraminiferal average living depth in the 0–10 cm sediment core

Station	Total abundance (ind. 63.5 cm^{-2})	Species richness (*S*)	ALD_{10} (cm)	Shannon index (*H*)	Evenness index (*E*)
A02	1940	8	2.5	1.09	0.37
C05	1180	14	2.4	2.02	0.54
M7	3022	25	1.4	1.52	0.18
F11	355	15	4.5	2.12	0.55
B5	1026	16	2.4	2.24	0.58
ME3	2868	22	5.1	1.68	0.24

stations and at Stns M7, ME3, and B5 was >3-fold that of the $PWNO_3$ pool (Table 5).

Total potential foraminiferal denitrification rate

The maximum and minimum potential benthic foraminiferal denitrification rates at each station are shown in Table 6. In the YS, the total potential foraminiferal denitrification rates ranged from 15 to 88 μmol m^{-2} d^{-1}, and it ranged from 9 to 92 μmol m^{-2} d^{-1} in the ECS. Stns C05, B5, and ME3 had relatively high potential foraminiferal denitrification rates, while the minimum rate (9–10 μmol m^{-2} d^{-1}) was found for Stn F11. *Fursenkoina schreibersiana* was responsible for most of the potential foraminiferal denitrification at Stns C05 and B5. The $TFDR_{max}$ were all <2-fold the $TFDR_{min}$ at each station except M7.

DISCUSSION

Vertical distribution of benthic foraminifera in sediments

Food supply as one of the most significant factors controls the dynamics and composition of benthic foraminiferal assemblage (Jorissen et al. 1998, Schmiedl et al. 2000). The chl *a* concentrations, CPE, and chl *a*:Phaeo ratio were all significantly positively correlated with the foraminiferal abundance (Pearson correlation: r = 0.595, 0.414, and 0.585, respectively; $p < 0.01$; n = 60), which indicated that the phytodetritus content and freshness were key factors affecting the vertical distribution of foraminifera in sediments of the YS and the ECS. However, foraminiferal abundance was uncorrelated with TOC in sediment (Figs. 3 & 5), which implies TOC may not be an ideal indicator to reflect food supply for benthic foraminifera. In the YS and the ECS, TOC as bulk organic carbon may con-

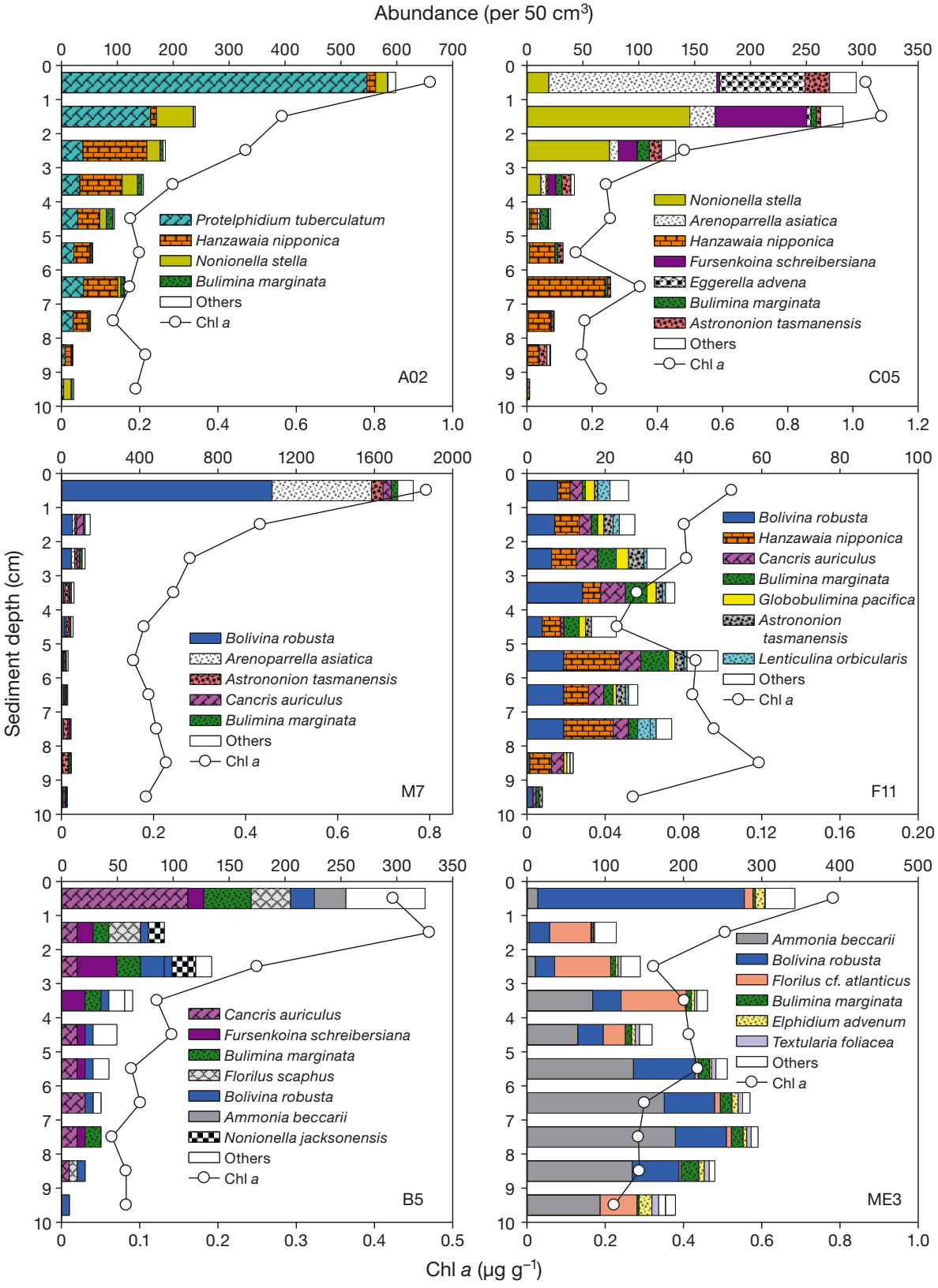

Fig. 5. Vertical abundances (individuals per 50 cm^3) of the dominant live foraminifera species (>2% for each station) in the >150 µm fraction, and the profiles of the chlorophyll *a* (chl *a*) concentrations

Table 5. Inventories of the $PWNO_3$ pool, $FINO_3$ pool, and $ICNO_3$ pool in sediments at each station. $PWNO_3$: pore water nitrate; $FINO_3$: foraminiferal intracellular nitrate; $ICNO_3$: intracellular nitrate

Station	$PWNO_3$ ($\mu mol\ m^{-2}$)	$FINO_3$ ($\mu mol\ m^{-2}$)	$ICNO_3$ ($\mu mol\ m^{-2}$)	Percentage of $FINO_3$ of $ICNO_3$	Ratio of $ICNO_3$ to $PWNO_3$
A02	148	31 ± 21	141	22	1.0
C05	209	35 ± 6	241	15	1.2
M7	77	138 ± 39	333	41	4.3
F11	153	34 ± 10	195	27	1.3
B5	59	159 ± 63	215	74	3.6
ME3	147	50 ± 14	579	9	3.9

Table 6. Minimum and maximum total potential foraminiferal denitrification rates at 6 sites

Station	Minimum rates ($\mu mol\ m^{-2}\ d^{-1}$)	Maximum rates ($\mu mol\ m^{-2}\ d^{-1}$)
Yellow Sea		
A02	15.60	25.62
C05	62.01	87.83
M7	15.02	60.01
East China Sea		
F11	9.23	10.45
B5	57.26	92.27
ME3	63.72	69.23

tain large amounts of refractory organic matter unavailable for benthic foraminifera in sediment, which was consistent with the low values of chl *a*:Phaeo in our study. Chl *a* and CPE as more labile parts of TOC in sediments might be more suitable for indicating food supply to benthic foraminifera.

Redox condition in sediments also affects the vertical distribution of benthic foraminifera (Jorissen et al. 1995, Fontanier et al. 2008). Many foraminiferal species were proven to rely on respiring $ICNO_3$ instead of oxygen in anoxic sediments (Risgaard-Petersen et al. 2006, Piña-Ochoa et al. 2010a, Bernhard et al. 2012). Our results agree with the previous publications. Foraminiferal abundance mainly peaked in surface oxic sediments at most stations (except Stn F11), which indicates most foraminifera were inclined to carry on aerobic metabolism. However, many specific foraminiferal species occurred below the OPD and even below NPD (Figs. 2 & 5), and nitrate storage was also encountered in some foraminiferal species (Table 2), which implies the potential foraminiferal anaerobic metabolism in anoxic sediments.

Arenoparella asiatica was mainly concentrated in the top 1 cm of sediments having almost the highest concentrations of chl *a* and CPE at Stns C05 and M7 (Figs. 4 & 5). *A. asiatica* also lacked cytoplasmic nitrate enrichment (Table 2), indicating that *A. asiatica* may rely on aerobic respiration in surface sediments having sufficient food sources. Although a small number of *A. asiatica* was present down to 3–4 cm depth in sediments at Stns C05 and M7, Rose Bengal staining is not very reliable in anoxic sediments and may also stain dead foraminiferal cytoplasm weeks to months after death (Bernhard 1988, Hannah & Rogerson 1997).

Nonionella stella was found to store high concentrations of $ICNO_3$ (Table 2), and the maximum abundance of *N. stella* in the sub-surface sediment layer at Stns C05 and A02 was below the OPD and above the NPD with relatively high concentrations of chl *a* and CPE (Figs. 2, 4 & 5). These conditions enabled *N. stella* to absorb nitrate from the adjacent pore water and to obtain sufficient food resources. In addition, *N. stella* is tolerant of low oxygen conditions and has been reported to denitrify at a rate of 84 ± 33 pmol $ind.^{-1}\ d^{-1}$ in the Chile oxygen minimum zone (OMZ) (Risgaard-Petersen et al. 2006) and to dominate the assemblages in Santa Barbara Basin anoxic sediments (Bernhard et al. 1997); $ICNO_3$ may provide the electron acceptor necessary for denitrification in anoxic sediments.

Fursenkoina schreibersiana had a similar vertical distribution to that of *N. stella* and occurred in anoxic sediments with relatively high concentrations of chl *a* and CPE at Stns C05 and B5. In the same genus, *Fursenkoina cornuta* from the Santa Barbara Basin was reported to enrich nitrate intracellularly and to have a high denitrification rate (Bernhard et al. 2012), and *Fursenkoina* sp. also occurs below the OPD in the Nazaré canyon on the Portuguese continental margin (Koho et al. 2007). We concluded *F. schreibersiana* may also use the same mechanism to colonize anaerobic sediments in the YS and the ECS.

Hanzawaia nipponica was present at 4–10 cm depth in sediments from Stn C05 and was also present in the deep sediment layer below the OPD and NPD at Stns A02, F11, and ME3 (ALD_{10} 4.3, 5.1, and 5.8 cm, respectively). *H. nipponica* was reported to store a high concentration of $ICNO_3$ (11 ± 3 mM), which is several thousand-fold that of the ambient pore water (Table 2). Koho et al. (2011) reported deep infaunal foraminiferal species collected nitrate by migrating up to NPD. Due to the deep ALD_{10} of *H. nipponica*, we suggested that the $ICNO_3$ of *H. nip-*

ponica (316 ±73 pmol ind^{-1}) may supply sufficient nitrate to support anaerobic respiration (denitrification) in anaerobic and nitrate-free sediments (i.e. below the NPD). In addition, *Hanzawaia nitidula* was reported to tolerate low oxygen conditions in the OMZ on the shelf of the Gulf of Tehuantepec and displayed more and larger pores than specimens from oxygenated waters (Perez-Cruz & Machain-Castillo 1990). We found *H. nipponica* (Fig. S3 in the Supplement) displayed larger but fewer pores than *H. nitidula* sampled in the OMZ (Perez-Cruz & Machain-Castillo 1990). Glock et al. (2011) also implied that the pores in *Bolovina spissa* may be related to the uptake of nitrate for denitrification.

Bolivina robusta dominated at Stns M7 and ME3, accounting for 60 and 77% of the total foraminiferal community in the top 1 cm (abundances of 1257 and 698 per 50 cm^2, respectively; Fig. 5). The occurrence of this genus in continental shelf settings appears to be opportunistic and apparently related to the availability of labile organic matter (Langezaal et al. 2006); this is consistent with the finding that the maximum chl *a* concentration, CPE, and chl *a*:Phaeo ratio occurred in the surface sediments at Stns M7 and ME3 (Figs. 4 & 5).

Bulimina marginata was present at all stations in our study, but its vertical distribution varied. *B. marginata* has been reported to be widely distributed (Koho et al. 2007) and to inhabit hypoxic and anoxic sediments as well as shallow oxic sediments (Rathburn & Corliss 1994, Bernhard & Alve 1996, Ohga & Kitazato 1997, Schönfeld 2001, Alve 2003). There have also been several reports of genus *Bulimina* occupying extremely eutrophic environments (Lutze & Coulbourn 1984, Jorissen 2003); we speculated eutrophication of the YS and the ECS may provide favorable conditions for *B. magrinata*.

Widespread occurrence of $ICNO_3$ storage (including benthic foraminifera) in sediments of the YS and the ECS

The ability among foraminifera to store nitrate has been reported for diverse benthic marine environments (Risgaard-Petersen et al. 2006, Høgslund et al. 2008, Glud et al. 2009, Piña-Ochoa et al. 2010a, Bernhard et al. 2012). Five foraminiferal species (*H. nipponica*, *N. stella*, *B. robusta*, *Cancris auriculus,* and *Globobulimina pacifica*) from the YS and the ECS were also found to store nitrate intracellularly at high concentrations ranging from 3 to 114 mM, which was >3 orders of magnitude higher than that of the surrounding pore water (Table 2, Fig. 2). Among the 5 species, *H. nipponica* is a new foraminiferal genus reported to store nitrate. $ICNO_3$ content in *B. robusta* (212 ± 46 pmol ind.$^{-1}$) is well within the range of values reported for genus *Bolivina* (83–1081 pmol ind.$^{-1}$; Piña-Ochoa et al. 2010a), and reports of nitrate content in *N. cf. stella* (186 ± 25 pmol ind.$^{-1}$; Risgaard-Petersen et al. 2006) were comparable to *N. stella* (162 ± 27 pmol ind.$^{-1}$). *Cancris auriculus* had the highest $ICNO_3$ concentration in our study (3211 ± 1046 pmol ind.$^{-1}$; 114 ± 23 mM), and the related species *C. inflatus* has been reported to have the highest $ICNO_3$ concentration so far (262 877 ± 4253 pmol ind.$^{-1}$; 262 ± 37 mM; Piña-Ochoa et al. 2010a), vastly exceeding that by *C. auriculus*. This suggests that nitrate storage may be a characteristic of the genus *Cancris*. The size of *C. inflatus* is much larger (0.12 ± 0.024 mm^3) than *C. auriculus* (0.028 ± 0.0051 mm^3), which may account for their relative abilities to store $ICNO_3$, and Glud et al. (2009) also suggested a size-dependent relationship for the variable $ICNO_3$ concentrations in *Globobulimina affinis*. Furthermore, *C. auriculus* accounted for 60% and 86% of the $FINO_3$ at Stns M7 and B5 respectively, and the $FINO_3$ concentrations at Stns M7 and B5 far exceeded that for $PWNO_3$ (Table 5). Similar findings have been reported for the Peruvian OMZ, where *C. inflatus* contributed large amounts of $ICNO_3$ (Glock et al. 2013). Our result also suggested the $FINO_3$ pool contributed to the $ICNO_3$ storage in sediments of the ESC, which was implied by Song et al. (2013).

In addition to benthic foraminifera, many prokaryotic and eukaryotic organisms (sulfur bacteria, diatoms, dinoflagellates, haptophytes, chlorophytes, and *Gromiids*) were also reported to store high concentrations of $ICNO_3$, and they might be also significant portions of the $ICNO_3$ pool in sediment (Dortch et al. 1984, Fossing et al. 1995, Lomas & Glibert 2000, Piña-Ochoa et al. 2010a, Kamp et al. 2011, 2015). The $ICNO_3$ concentrations have been measured using various extraction methods (e.g. Sayama 2001, Risgaard-Petersen et al. 2006, Prokopenko et al. 2011, Larsen et al. 2013). To assess the most effective method for releasing $ICNO_3$, we compared various extraction methods using samples collected at Stn ME3. Amongst all methods, the Frozen extraction method produced the highest nitrate concentrations for most of the sediment layers analyzed, suggesting that this may be the most effective method for analysis of $ICNO_3$ (Fig. 2).

The inventory of the $ICNO_3$ pool was greater than that of the $PWNO_3$ pool at most stations, and the ratios $ICNO_3$ pool to $PWNO_3$ pool ranged from 1 to 4.3 (Table 5). Even though the ratios were lower than

the reported values in previous publications (4 to 26) (Glud et al. 2009, Prokopenko et al. 2011, Glock et al. 2013, Larsen et al. 2013), the $ICNO_3$ pool independent of the $PWNO_3$ pool was still an important nitrate pool in sediments of the YS and the ECS. $ICNO_3$ concentrations in sediments always changed accompanied by $PWNO_3$, and decreased with sediment depth (Fig. 2), indicating that $ICNO_3$ may be absorbed from $PWNO_3$ above the NPD.

The percentage of $FINO_3$ pool relative to $ICNO_3$ pool showed large variation, and only at Stn B5 did the $FINO_3$ pool account for >50% of the $ICNO_3$ pool. This suggests that organisms in addition to foraminifera may also contribute significantly to the potential nitrate pool in sediments. Sediments of the ECS contain abundant resting stage diatom cells of *Skeletonema* (Zhang et al. 2010), which store high $ICNO_3$ concentrations (11 mM; Kamp et al. 2011). The chl *a*, CPE, and chl *a*:Phaeo ratio were all significantly positively correlated with the $ICNO_3$ concentrations (Pearson correlation: r = 0.563, 0.603, and 0.457, respectively; $p < 0.01$; n = 60), which indicated that the phytodetritus (e.g. diatoms) may also play an important role in nitrate storage in sediments of the YS and the ECS.

The maximum level of $ICNO_3$ storage always associated with near-surface sediments (Fig. 2), the foraminiferal abundance and chl *a* concentration both peaked in near-surface sediment (except at Stn F11) (Fig. 5). We suggested benthic foraminifera and phytodetritus (e.g. diatoms) may both contributed to the maximum concentration of $ICNO_3$ in near-surface sediments. At Stns M7 and ME3, large amounts of $ICNO_3$ occurred below the NPD. Burial of diatoms may remove them several centimetres or decimetres into the sediment (Heisterkamp et al. 2012). $ICNO_3$ below the NPD might be caused by the presence of diatoms in deep sediment layers. Furthermore, deep infaunal foraminifera were found at these stations. Benthic foraminifera are able to migrate between nitrate-containing and nitrate-free layers in sediments to collect $ICNO_3$ (Koho et al. 2011). We suggested a part of the $ICNO_3$ below NPD may be also caused by the $FINO_3$, and the deep infaunal foraminifera may collect nitrate in nitrate-containing layers and migrate to nitrate-free layers in sediments, which might also promote nitrogen loss and decrease the efficiency of organic carbon burial (Prokopenko et al. 2011, Dale et al. 2016).

Many of the foraminiferal species present in anoxic sediments were not included in the analysis of $ICNO_3$ and so were not taken into account in our calculations; this suggests that the $FINO_3$ may have been underestimated. For instance, *Ammonia beccarii*, which dominated at Stn ME3, was unaccounted in calculations, but Nomaki et al. (2015) have reported *Ammonia* sp. enriched $ICNO_3$ (80 pmol ind.$^{-1}$). The $ICNO_3$ concentrations were positively correlated with foraminiferal abundance in every sediment layer analyzed (Pearson correlation; r = 0.3847, p = 0.0014, n = 60), indicating a close link between the abundance of foraminifera and the $ICNO_3$ content. The results also implied that benthic foraminifera may play a significant role in nitrate storage in sediments of the YS and the ECS.

Role of benthic foraminifera in nitrogen removal from sediments in the YS and the ESC

Foraminiferal denitrification as a newly recognized pathway for nitrogen loss has mainly been studied in low oxygen marine areas, and there has been little research in oxic continental shelf areas. The potential foraminiferal denitrification rates in the YS and the ECS ranged from 9 to 92 µmol N m^{-2} d^{-1} (Table 6). Due to high abundance and high individual denitrification rate, *F. schreibersiana* contributed most of the potential foraminiferal denitrification at Stns C05 and B5. *F. cornuta* was also reported to play a role in the sedimentary denitrification of the Santa Barbara Basin (Bernhard et al. 2012). The potential foraminiferal denitrification rate was lowest at Stn F11, which also had the lowest foraminferal abundance. The particularly low chl *a* concentration and chl *a*:Phaeo ratio at this station manifested the lack of available labile organic matter as food for foraminifera. Our estimates include some uncertainty because the foraminiferal species-specific denitrification rates we found may not represent the rates in situ, and foraminifera smaller than 150 µm were not taken into account. In addition, considering oxic bottom water and surface oxic sediments may inhibit denitrification, we calculated the $TFDR_{max}$ and the $TFDR_{min}$ respectively at each station (Table 6). Only at Stn M7 was the $TFDR_{max}$ more than twice of the $TFDR_{min}$, because large numbers of denitrifying species *B. robusta* (Fig. 5) occurred in the 0–1 cm sediment layer.

We compared the potential foraminiferal denitrification rates in the YS and the ESC with those reported from diverse benthic marine environments, to assess the factors underpinning the differences (Table 7). The potential foraminiferal denitrification rates in the YS and the ECS were comparable to the rates estimated for Sagami Bay (Glud et al. 2009) and the Bay of Biscay (Piña-Ochoa et al. 2010a), were

Table 7. Total and foraminiferal denitrification rates in sediments from diverse benthic marine environments

Total denitrification rates (μmol N m^{-2} d^{-1})	Foraminiferal denitrification rates (μmol N m^{-2} d^{-1})	Percentage	Sites	Near-bottom water DO (μM)	Source
1030	720	70%	Skagerrak, Sweden	300	Piña-Ochoa et al. (2010a)
76	64	84%	Bay of Biscay, France	200	Piña-Ochoa et al. (2010a)
250	173	70%	OMZ, Chile	<1	Piña-Ochoa et al. (2010a)
900[a]	420	47%	79 m, OMZ, Peru	1	Glock et al. (2013)
3800[a]	1320	35%	248 m, OMZ, Peru	1	Glock et al. (2013)
3200[a]	550	17%	319 m, OMZ, Peru	1	Glock et al. (2013)
700[a]	13	2%	697 m, OMZ, Peru	13	Glock et al. (2013)
510-840	78	9–15%	OMZ, Arabian Sea	<1	Piña-Ochoa et al. (2010a)
4500	3000	67%	Santa Barbara Basin, American	0–15	Bernhard et al. (2012)
720	50	4%	Sagami Bay, Japan	55–60	Glud et al. (2009)
120	1–13	1–11%	Jones Bank, Celtic Sea	267	Larsen et al. (2013)
264[b]	64–69	24–26%	ME3, East China Sea	159	This study
45[c]	16–26	36–58%	A02, Yellow Sea	213	This study
144[c]	62–88	43–61%	C05, Yellow Sea	220	This study

[a]Total benthic nitrate loss; [b]Data from Song et al. 2016b; [c]Data from Song et al. (unpubl. data)

slightly higher than for Jones Bank in the Celtic Sea (Larsen et al. 2013), and were less than for low-oxygen marine areas including the Chilean OMZ (Piña-Ochoa et al. 2010a), the Peruvian OMZ (Glock et al. 2013), and the Santa Barbara Basin (Bernhard et al. 2012). Foraminiferal aerobic respiration yields more energy (generally a factor of 3 to 13 higher) than denitrification (Strohm et al. 2007, Piña-Ochoa et al. 2010a), and oxygen is the first choice for benthic foraminifera to respire in oxic marine environment. The bottom water in the YS and the ECS is commonly aerobic (Table 1), so the surface oxic sediments will not support anaerobic respiration by benthic foraminifera. However, the highest foraminiferal abundance was mainly present in near-surface sediments (Fig. 5), and potential foraminiferal denitrification in the YS and the ECS will only occur in the sediments below the depth to which oxygen penetrates, accompanied by $ICNO_3$ storage (Fig. 2). In contrast, the surface sediments in the Chilean and Peruvian OMZs and the Santa Barbara Basin are long-term anaerobic environments in which benthic foraminifera and prokaryotes including *Thioploca* and *Beggiatoa* thrive in the surface anoxic sediments (Mosch et al. 2012). Glock et al. (2013) reported potential foraminiferal denitrification rates showed maximum values in the centre of the Peruvian OMZ and decreased rapidly with increasing bottom water DO at different stations. The bottom DO concentration may be a key factor controlling potential foraminiferal denitrification rates. Furthermore, most organic carbon derived from primary productivity is decomposed in well-oxygenated seawater, and only approximately 10% and 30% of the particulate organic carbon settles to the sediments in the YS and the ECS, respectively (Song et al. 2016a). This is consistent with the low chl *a*:Phaeo ratio at stations in our study, which also reflects the lack of fresh organic matter, and the highest chl *a* concentration, CPE and chl *a*:Phaeo ratio mainly occurred in the near-surface oxic sediments. However, the chl *a* concentrations, CPE, chl *a*:Phaeo ratio, and TOC values in the sediments of the Chilean and Peruvian OMZs far exceed those in the YS and the ECS (Gallardo et al. 2004, Cardich et al. 2015), potentially reflecting the sufficient supply of organic matter for foraminifera. Therefore, the abundance of denitrifying foraminiferal species in the YS and the ECS is not as high as in Chilean and Peruvian OMZs (Høgslund et al. 2008, Piña-Ochoa et al. 2010a, Bernhard et al. 2012, Glock et al. 2013). The oxygen concentration and food availability may both have contributed to the relative low potential foraminiferal denitrification rates in the YS and the ECS.

Limited information about the total denitrification rates was reported in sediments of the YS and the ECS. To evaluate the potential importance of foraminiferal denitrification in sediments, the total denitrification rate at Stn ME3 referred to the result of the closest station DH61 (264 μmol m^{-2} d^{-1}) reported by Song et al. (2016b). At Stns A02 and C05, the total denitrification rates were obtained at the same stations (A02 and C05) of the same cruise with this study. The determination method was based on application of the ^{15}N isotope pairing technique (Nielsen 1992) in intact core incubations, and the calculation method referred to Song et al. (2016b) modified from Ris-

gaard-Petersen et al. (2003). The total denitrification rates were 45 and 144 µmol m^{-2} d^{-1} at Stns A02 and C05 respectively (G. Song et al. unpubl. data). Dividing the minimum or maximum potential foraminiferal denitrification rates (Table 6) by total denitrification rates above, approximately 36–58%, 43–61%, and 24–26% of the total denitrification rates were attributable to benthic foraminifera at Stns A02, C05, and ME3 respectively (Table 7), indicating that they might play a role in sedimentary denitrification of the YS and the ECS.

CONCLUSIONS

Five foraminiferal species *Nonionella stella*, *Hanzawaia nipponica*, *Bolivina robusta*, *Cancris auriculus*, and *Globobulimina pacifica* contained high concentrations of nitrate, sometimes exceeding the levels in the adjacent pore waters by >3 orders of magnitude. Sediment redox conditions and phytodetritus content and freshness were key factors deciding the vertical distribution of benthic foraminifera in the YS and ECS. A widespread $ICNO_3$ pool occurred in sediments of the YS and the ECS, and the inventory of the $FINO_3$ pool ranged from 31 to 159 µmol m^{-2}, which exceeded that of the $PWNO_3$ pool at Stns B5 and M7. The $FINO_3$ pool as a proportion of the $ICNO_3$ pool ranged from 9 to 74%, and the $ICNO_3$ concentration correlated well with the foraminiferal abundance, suggesting that benthic foraminifera constitute an important nitrate reservoir. The chl *a* concentrations, CPE, and chl *a*:Phaeo ratio were all significantly positively correlated with the $ICNO_3$ concentrations (Pearson correlation: $r = 0.563$, 0.603 and 0.457, respectively; $p < 0.01$; $n = 60$); we suggested the phytodetritus (e.g. diatoms) may also contribute to nitrate storage in sediments. The potential foraminiferal denitrification rates ranged from 9 to 92 µmol N m^{-2} d^{-1} in the YS and the ECS, which indicates that benthic foraminifera might play a role in the sedimentary denitrification of the YS and the ECS.

Acknowledgements. This work was supported by the Ministry of Science & Technology of PR China (2011CB409802) and the National Science Foundation of China (40925017, 41521064), Aoshan Talents Program Supported by Qingdao National Laboratory for Marine Science and Technology (No. 2015ASTP-OS08), and the Taishan Scholars Program of Shandong Province. The authors thank the captains and crews of the R/V 'Dongfanghong 2'. We also sincerely thank Xiaoyan Ning, Xuming Kang, Lingyan Wang, Shuhang Dong and Bin Yang for their help in field studies.

LITERATURE CITED

Alve EA (2003) Common opportunistic foraminiferal species as an indicator of rapidly changing conditions in a range of environments. Estuar Coast Shelf Sci 57:501–514

Arrigo KR (2005) Marine microorganisms and global nutrient cycles. Nature 437:349–355

Bernhard JM (1988) Postmortem vital staining in benthic foraminifera; duration and importance in population and distributional studies. J Foraminiferal Res 18:143–146

Bernhard JM (1992) Benthic foraminiferal distribution and biomass related to pore-water oxygen content: central California continental slope and rise. Deep Sea Res A 39: 585–605

Bernhard JM (2000) Distinguishing live from dead foraminifera: methods review and proper applications. Micropaleontology 46:38–46

Bernhard JM, Alve E (1996) Survival, ATP pool, and ultrastructural characterization of benthic foraminifera from Drammensfjord (Norway): response to anoxia. Mar Micropaleontol 28:5–17

Bernhard JM, Gupta BKS, Borne PF (1997) Benthic foraminiferal proxy to estimate dysoxic bottom-water oxygen concentrations: Santa Barbara Basin, U.S. Pacific continental margin. J Foraminiferal Res 27:301–310

Bernhard JM, Casciotti KL, McIlvin MR, Beaudoin DJ, Visscher PT, Edgcomb VP (2012) Potential importance of physiologically diverse benthic foraminifera in sedimentary nitrate storage and respiration. J Geophys Res Biogeosci 117:G03002

Braman RS, Hendrix SA (1989) Nanogram nitrite and nitrate determination in environmental and biological-materials by vanadium (III) reduction with chemiluminescence detection. Anal Chem 61:2715–2718

Cardich J, Gutiérrez D, Romero D, Pérez A and others (2015) Calcareous benthic foraminifera from the upper central Peruvian margin: control of the assemblage by pore water redox and sedimentary organic matter. Mar Ecol Prog Ser 535:63–87

Corliss BH (1985) Microhabitats of benthic foraminifera within deep-sea sediments. Nature 314:435–438

Corliss BH, Emerson S (1990) Distribution of Rose Bengal stained deep-sea benthic foraminifera from the Nova Scotian continental margin and Gulf of Maine. Deep Sea Res A 37:381–400

Dale AW, Sommer S, Lomnitz U, Bourbonnais A, Wallmann K (2016) Biological nitrate transport in sediments on the Peruvian margin mitigates benthic sulfide emissions and drives pelagic N loss during stagnation events. Deep Sea Res I 112:123–136

Dortch Q, Clayton JR Jr, Thoresen SS, Ahmed SI (1984) Species differences in accumulation of nitrogen pools in phytoplankton. Mar Biol 81:237–250

Fontanier C, Jorissen FJ, Lansard B and others (2008) Live foraminifera from the open slope between Grand Rhône and Petit Rhône Canyons (Gulf of Lions, NW Mediterranean). Deep Sea Res I 55:1532–1553

Gallardo VA, Palma M, Carrasco FD, Gutiérrez D, Levin LA, Cañete, JI (2004) Macrobenthic zonation caused by the oxygen minimum zone on the shelf and slope off central Chile. Deep Sea Res II 51:2475–2490

Fossing H, Gallardo VA, Jørgensen BB, Hüttel M, and others (1995) Concentration and transport of nitrate by the mat-forming sulfur bacterium *Thioploca.* Nature 374: 713–715

Glock N, Eisenhauer A, Milker Y, Liebetrau V, and others (2011) Environmental influences on the pore density of *Bolivina spissa* (Cushman). J Foraminiferal Res 41:22–32

Glock N, Schönfeld J, Eisenhauer A, Hensen C, Mallon J, Sommer S (2013) The role of benthic foraminifera in the benthic nitrogen cycle of the Peruvian oxygen minimum zone. Biogeosciences 10:4767–4783

Glud RN, Thamdrup B, Stahl H, Wenzhoefer F (2009) Nitrogen cycling in a deep ocean margin sediment (Sagami Bay, Japan). Limnol Oceanogr 54:723–734

Gong GC, Wen YH, Wang BW, Liu GJ (2003) Seasonal variation of chlorophyll a concentration, primary production and environmental conditions in the subtropical East China Sea. Deep Sea Res II 50:1219–1236

Gooday AJ (1986) Meiofaunal foraminiferans from the bathyal Porcupine Seabight (north-east Atlantic): size structure, standing stock, taxonomic composition, species diversity and vertical distribution in the sediment. Deep Sea Res A 33:1345–1373

Gooday AJ, Bernhard JM, Levin LA, Suhr SB (2000) Foraminifera in the Arabian Sea oxygen minimum zone and other oxygen-deficient settings: taxonomic composition, diversity, and relation to metazoan faunas. Deep Sea Res II 47:25–54

Gruber N (2004) The dynamics of the marine nitrogen cycle and its influence on atmospheric CO_2 variations. In: Follows M, Oguz T (eds) The ocean carbon cycle and climate. Springer, Dordrecht, p 97–148

Guan B (1994) Patterns and structures of the currents in Bohai, Huanghai and East China Seas. In: Di Z, Yuanbo L, ChengKui Z (eds) Oceanology of China Seas, Vol 1. Kluwer Academic Publishers, Dordrecht, p 17–26

Hannah F, Rogerson A (1997) The temporal and spatial distribution of foraminiferans in marine benthic sediments of the Clyde Sea area, Scotland. Estuar Coast Shelf Sci 44:377–383

Hayek LEC, Buzas MA (1997) Surveying natural populations. Colombia University Press, New York, NY

Heisterkamp IM, Kamp A, Schramm AT, de Beer D, Stief P (2012) Indirect control of the intracellular nitrate pool of intertidal sediment by the polychaete *Hediste diversicolor*. Mar Ecol Prog Ser 445:181–192

Høgslund S, Revsbech NP, Cedhagen T, Nielsen LP, Gallardo VA (2008) Denitrification, nitrate turnover, and aerobic respiration by benthic foraminiferans in the oxygen minimum zone off Chile. J Exp Mar Biol Ecol 359:85–91

Hu LM, Shi XF, Yu ZG, Lin T and others (2012) Distrbution of sedimentary organic matter in estuarine–inner shelf regions of the East China Sea: implications for hydrodynamic forces and anthropogenic impact. Mar Chem 142-144:29–40

Humborg C, Ittekkot V, Cociasu A, Bodungen BV (1997) Effect of Danube River dam on Black Sea biogeochemistry and ecosystem structure. Nature 386:385–388

Jorissen FJ (2003) Benthic foraminiferal microhabitats below the sediment-water interface. In: Gupta BKS (ed) Modern foraminifera. Springer, Dordrecht, p 161–179

Jorissen FJ, de Stigter HC, Widmark JGV (1995) A conceptual model explaining benthic foraminiferal microhabitats. Mar Micropaleontol 26:3–15

Jorissen FJ, Wittling I, Peypouquet JP, Rabouille C, Relexans JC (1998) Live benthic foraminiferal faunas off Cape Blanc, NW-Africa: community structure and microhabitats. Deep Sea Res I 45:2157–2188

Kamp A, de Beer D, Nitsch JL, Lavik G, Stief P (2011) Diatoms respire nitrate to survive dark and anoxic conditions. Proc Natl Acad Sci USA 108:5649–5654

Kamp A, Høgslund S, Risgaard-Petersen N, Stief P (2015) Nitrate storage and dissimilatory nitrate reduction by eukaryotic microbes. Front Microbiol 6:1492

Koho KA, Piña-Ochoa E (2012) Benthic foraminifera: inhabitants of low-oxygen environments. Anoxia, Springer, Dordrecht, p 249–285

Koho KA, Kouwenhoven TJ, De Stigter HC, Van Der Zwaan GJ (2007) Benthic foraminifera in the Nazaré Canyon, Portuguese continental margin: sedimentary environments and disturbance. Mar Micropaleontol 66:27–51

Koho KA, Piña-Ochoa E, Geslin E, Risgaard-Petersen N (2011) Vertical migration, nitrate uptake and denitrification: survival mechanisms of foraminifers (*Globobulimina turgida*) under low oxygen conditions. FEMS Microbiol Ecol 75: 273–283

Langezaal AM, Jorissen FJ, Braun B, Chaillou G, Fontanier C, Anschutz P, Van der Zwaan GJ (2006) The influence of seasonal processes on geochemical profiles and foraminiferal assemblages on the outer shelf of the Bay of Biscay. Cont Shelf Res 26:1730–1755

Larsen M, Thamdrup B, Shimmield T, Glud RN (2013) Benthic mineralization and solute exchange on a Celtic Sea sand-bank (Jones Bank). Prog Oceanogr 117:64–75

Liu SM, Hong GH, Zhang J, Ye XW, Jiang XL (2009) Nutrient budgets for large Chinese estuaries. Biogeosciences 6:2245–2263

Liu SM, Li LW, Zhang Z (2011) Inventory of nutrients in the Bohai. Cont Shelf Res 31:1790–1797

Lomas MW, Glibert PM (2000) Comparisons of nitrate uptake, storage, and reduction in marine diatoms and flagellates. J Phycol 36:903–913

Lutze GF, Coulbourn WT (1984) Recent benthic foraminifera from the continental margin of northwest Africa: community structure and distribution. Mar Micropaleontol 8: 361–401

Middelburg JJ, Soetaert K, Herman PMJ, Heip CHR (1996) Denitrification in marine sediments: a model study. Global Biogeochem Cycles 10:661–673

Mosch T, Sommer S, Dengler M, Noffke A and others (2012) Factors influencing the distribution of epibenthic megafauna across the Peruvian oxygen minimum zone. Deep Sea Res I 68:123–135

Murray JW (2006) Ecology and applications of benthic foraminifera. Cambridge University Press, New York, NY

Nielsen LP (1992) Denitrification in sediment determined from nitrogen isotope pairing. FEMS Microbiol Ecol 86:357–362

Nomaki H, Chikaraishi Y, Tsuchiya M, Toyofuku T and others (2015) Variation in the nitrogen isotopic composition of amino acids in benthic foraminifera: implications for their adaptation to oxygen-depleted environments. Limnol Oceanogr 60:1906–1916

Ohga T, Kitazato H (1997) Seasonal changes in bathyal foraminiferal populations in response to the flux of organic matter (Sagami Bay, Japan). Terra Nova 9:33–37

Perez-Cruz LL, Machain-Castillo ML (1990) Benthic foraminifera of the oxygen minimum zone, continental shelf of the Gulf of Tehuantepec, Mexico. J Foraminiferal Res 20: 312–325

Piña-Ochoa E, Høgslund S, Geslin E, Cedhagen T and others (2010a) Widespread occurrence of nitrate storage and denitrification among Foraminifera and *Gromiida*. Proc Natl Acad Sci USA 107:1148–1153

Piña-Ochoa E, Koho KA, Geslin E, Risgaard-Petersen N (2010b) Survival and life strategy of the foraminiferan *Globobulimina turgida* through nitrate storage and denitrification. Mar Ecol Prog Ser 417:39–49

Prokopenko MG, Sigman DM, Berelson WM, Hammond DE, Barnettet B, Chong L, Townsend-Small A (2011) Denitrification in anoxic sediments supported by biological nitrate transport. Geochim Cosmochim Acta 75:7180–7199

Rathburn AE, Corliss BH (1994) The ecology of living (stained) deep-sea benthic foraminifera from the Sulu Sea. Paleoceanography 9:87–150

Risgaard-Petersen N, Nielsen LP, Rysgaard S, Dalsgaard T, Meyer RL (2003) Application of the isotope pairing technique in sediments where anammox and denitrification coexist. Limnol Oceanogr Methods 1:63–73

Risgaard-Petersen N, Langezaal AM, Ingvardsen S, Schmid MC (2006) Evidence for complete denitrification in a benthic foraminifer. Nature 443:93–96

Sayama M (2001) Presence of nitrate-accumulating sulfur bacteria and their influence on nitrogen cycling in a shallow coastal marine sediment. Appl Environ Microbiol 67: 3481–3487

Schmiedl G, de Bovee F, Buscail R, Charriere B, Hemleben C, Medernach L, Picon P (2000) Trophic control of benthic foraminiferal abundance and microhabitat in the bathyal Gulf of Lions, western Mediterranean Sea. Mar Micropaleontol 40:167–188

Schönfeld J (2001) Benthic foraminifera and pore-water oxygen profiles: a reassessment of species boundary conditions at the western Iberian Margin. J Foraminiferal Res 31:86–107

Seeberg-Elverfeldt J, Schlüter M, Feseker T, Kölling M (2005) Rhizon sampling of porewaters near the sediment-water interface of aquatic systems. Limnol Oceanogr Methods 3:361–371

Seitzinger SP (1988) Denitrification in freshwater and coastal marine ecosystems: ecological and geochemical significance. Limnol Oceanogr 33:702–724

Shannon CE (1948) A mathematical theory of communication. Bell Syst Tech J 27:623–656

Shuman FR, Lorenzen CJ (1975) Quantitative degradation of chlorophyll by a marine herbivore. Limnol Oceanogr 20: 580–586

Song GD, Liu SM, Marchant H, Kuypers MMM, Lavik G (2013) Anammox, denitrification and dissimilatory nitrate reduction to ammonium in the East China Sea sediment. Biogeosciences 10:6851–6864

Song GD, Liu SM, Zhu ZY, Zhai WD, Zhu CJ, Zhang J (2016a) Sediment oxygen consumption and benthic organic carbon mineralization on the continental shelves of the East China Sea and the Yellow Sea. Deep Sea Res II 124:53–63

Song GD, Liu SM, Kuypers MMM, Lavik G (2016b) Application of the isotope pairing technique in sediments where anammox, denitrification, and dissimilatory nitrate reduction to ammonium coexist. Limnol Oceanogr Methods 14: 801–815

Strohm TO, Griffin B, Zumft WG, Schink B (2007) Growth yields in bacterial denitrification and nitrate ammonification. Appl Environ Microbiol 73:1420–1424

Thiel HJ (1978) Benthos in upwelling regions. In: Boje R, Tomczak M (ed) Upwelling ecosystems, Springer, Berlin, p 124–138

Turner RE, Rabalais NN (1994) Coastal eutrophication near the Mississippi river delta. Nature 368:619–621

Turner RE, Rabalais NN, Justic D, Dortch Q (2003) Global patterns of dissolved N, P and Si in large rivers. Biogeochemistry 64:297–317

Walton WR (1952) Techniques for recognition of living foraminifera. Contrib Cushman Found Foraminifer Res 3:56–60

Yentsch CS, Menzel DW (1963) A method for the determination of phytoplankton chlorophyll and phaeophytin by fluorescence. Deep Sea Res 10:221–231

Zhang J, Liu SM, Ren JL, Wu Y, Zhang GL (2007a) Nutrient gradients from the eutrophic Changjiang (Yangtze River) Estuary to the oligotrophic Kuroshio waters and re-evaluation of budgets for the East China Sea Shelf. Prog Oceanogr 74:449–478

Zhang J, Wu Y, Jennejahn TC, Ittekkot V, He Q (2007b) Distribution of organic matter in the Changjiang (Yangtze River) Estuary and their stable carbon and nitrogen isotopic ratios: implications for source discrimination and sedimentary dynamics. Mar Chem 106:111–126

Zhang Y, Lu S, Zhang C, Gao Y (2010) Distribution and germination of viable diatom resting stage cells in sediments of the East China Sea. Acta Oceanol Sin 29(5):121–128

Editorial responsibility: Ronald Kiene, Mobile, Alabama, USA

Submitted: August 15, 2016; Accepted: March 30, 2017
Proofs received from author(s): May 6, 2017